A Magnetic Harmonic Gear with Double Fan-Shaped Halbach Arrays

Xiaocun Huang[1] and Libing Jing[2, *]

Abstract—Compared with the conventional coaxial magnetic gear, magnetic harmonic gear (MHG) is a device with large transmission ratio. In order to improve the transmission torque, an MHG with double fan-shaped Halbach arrays is proposed in this paper. According to the theory of magnetic field modulation and the unique unilateral effect of Halbach array, both inner and outer permanent magnets (PMs) are arranged in a Halbach array. In addition, all PMs are fan-shaped. The air gap magnetic field and torque of MHG are analyzed by two-dimensional finite element method. Compared with the conventional MHG, the proposed MHG enhances the air-gap magnetic flux density, reduces the air-gap harmonic content, and increases the torque density.

1. INTRODUCTION

Magnetic gear is a kind of torque transmission device based on the principle of magnetic field modulation. In recent years, more and more scholars pay attention to magnetic gear [1, 2]. Compared with the conventional mechanical gear, the magnetic gear has many advantages, such as no friction, low vibration noise, no lubrication, overload protection, and less maintenance [3–5]. At present, magnetic gears have been applied in many low-speed and high torque occasions, especially in the combination with permanent magnet motor, such as wind power generator [6, 7], electric vehicles [8, 9], and ship electric propulsion [10, 11].

The concept of magnetic gears was first put forward by Brukwici in 1913. Although magnetic gear solves the problems of friction, lubrication, and noise of mechanical gear transmission in a certain sense, its practical application is seriously restricted due to low performance parameters such as remanence and maximum magnetic energy product of PM materials at that time. It was not until the appearance of NbFeB in 1980 that the research of magnetic gear was further explored. In 2001, a coaxial magnetic gear was proposed by Atallah and Howe, which uses a modulating ring to modulate the magnetic field in the inner and outer air gap, and the torque density can be up to $100 \, \text{kN·m/m}^3$ [12]. However, when the transmission ratio is greater than 20 : 1, the torque density will be significantly decreased.

In order to obtain the torque transmission with large transmission ratio, a magnetic harmonic gear (MHG) was proposed in 2007 [13]. The special structure is shown in Fig. 1. Not only is MHG suitable for transmission ratio over 20 : 1, but also the torque density is up to $150 \, \text{kN·m/m}^3$ [14]. In 2009, the concept of cycloidal magnetic gear is proposed [15]. Compared with coaxial magnetic gear, cycloidal magnetic gear has a large transmission ratio, and the output torque density is almost twice of that of coaxial magnetic gear. In [16], a fractional linear method is proposed to calculate the MHG model, and the air gap flux distribution of MHG is obtained by superposition principle. The calculated results are compared with the finite element analysis results, which show that the error of this method is small. In the field of permanent magnet magnetization, Halbach array has been widely used in the magnetic gear. The advantages of Halbach arrays are to improve the torque density and reduce the torque ripple [17–19]. In [20], an eccentric inner rotor pole and Halbach outer rotor pole are proposed and analyzed. The

[1] College of Physics and Information Engineering, Cangzhou Normal University, Cangzhou 061001, China. [2] College of Electrical Engineering & New Energy, China Three Gorges University, Yichang 443002, China.

eccentric structure of inner rotor permanent magnet is helpful for obtaining sinusoidal flux waveform and reduce torque ripple. The torque density can be up to $173\,\text{kN·m/m}^3$.

In this paper, an MHG with double fan-shaped Halbach arrays is proposed. The PMs on the low-speed rotor and stator are arranged in a fan-shape and magnetized by a Halbach array. The second part will introduce the principle, topology, and flux distributions of MHG. The torque of MHG will be calculated in the third part. The last part will draw a conclusion.

2. BASIC THEORY AND MAGNETIC FIELD ANALYSIS

2.1. Basic Theory of MHG

As shown in Fig. 1, MHG consists of the following 4 parts: bearing, high-speed rotor, low-speed rotor, and stator. The low-speed rotor is connected with the high-speed rotor through the bearing. The high-speed rotor and low-speed rotor rotate eccentrically relative to the stator, and the motion direction is the same. There is a sinusoidal time-varying air gap between the low-speed rotor and the stator. By modulating the magnetic field generated by two groups of permanent magnets, the pole pairs of asynchronous space magnetic flux density harmonics formed by one group of permanent magnets are equal to those of the other group of permanent magnets, so as to realize the transmission of torque and speed.
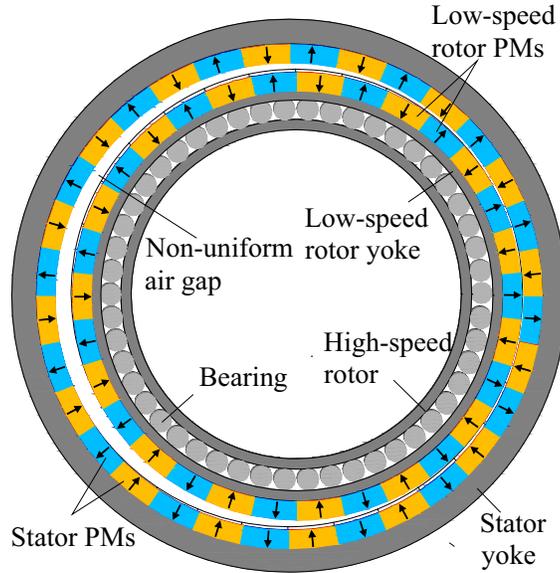
Figure 1. Conventional magnetic harmonic gear.

The length of nonuniform air gap between the low-speed rotor and the stator can be written as follows:

$$g = \frac{g_{\max} + g_{\min}}{2} + \left(\frac{g_{\max} - g_{\min}}{2} \right) \times \cos(p_\omega(\theta - \omega_h t)) \tag{1}$$

where $g_{\max}$ and $g_{\min}$ are the maximum and minimum values of air gap length, respectively; p_ω is the number of cycles of the non-uniform air gap, and ω_h is the angular velocity of the high-speed rotor.

Figure 2 shows the conventional MHG with two different air gap cycles. Due to the variable length of air gap, the magnetic field generated by two groups of PMs is modulated, so that one group of magnetic poles has the same number as the other group. When the high-speed rotor rotates around the stator center, the low-speed rotor rotates independently due to the coupling effect of the stator magnetic field.
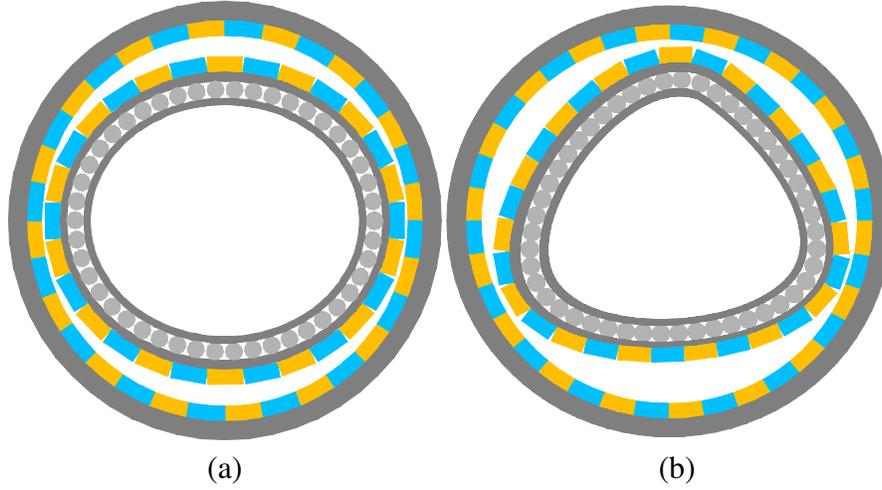
Figure 2. Conventional MHG with different air gap cycles. (a) $p_\omega = 2$; (b) $p_\omega = 3$.

At the radius distance r, the radial flux density distributions produced by the low-speed rotor permanent magnet can be written as follows:

$$
\begin{aligned}
B_r(r, \theta) &= \left(\sum_{m=1,3,5,\ldots} b_{rm}(r) \cos(mp(\theta - \omega_r t) + mp\,\theta_0) \right) \times [\lambda_0 + \lambda_1 \cos(p_\omega(\theta - \omega_h t))] \\
&= \sum_{m=1,3,5,\ldots} (b_{rm}(r) \cos(mp(\theta - \omega_r t) + mp\,\theta_0)\lambda_0) \\
&\quad + (b_{rm}(r) \cos(mp(\theta - \omega_r t) + mp\,\theta_0) \times \lambda_1 \cos(p_\omega(\theta - \omega_h t))) \\
&= \sum_{m=1,3,5,\ldots} (b_{rm}(r) \cos(mp(\theta - \omega_r t) + mp\,\theta_0)\lambda_0) \\
&\quad + \left(\frac{b_{rm}(r)\lambda_1}{2} \times \cos((mp - p_\omega)\theta + (p_\omega\omega_h - mp\,\omega_r)t + mp\,\theta_0) \right) \\
&\quad + \left(\frac{b_{rm}(r)\lambda_1}{2} \times \cos((mp + p_\omega)\theta - (p_\omega\omega_h + mp\,\omega_r)t + mp\,\theta_0) \right)
\end{aligned}
\tag{2}
$$

where p is the number of pole pairs of the low-speed rotor; ω_r is the angular velocity of the low-speed rotor; λ and λ_1 are constants, which are the first two Fourier coefficients of the modulation function, and their magnitude is related to the radial component of the magnetic flux density.

It can be seen from Equation (2) that the expression of pole pairs of space harmonic flux density generated by low-speed rotor permanent magnet can be expressed as:

$$
q_{m,k} = mp + (-1)^k p_\omega
\tag{3}
$$

where $m = 1, 3, 5\ldots, \infty$; $k = 1, 2$. According to the description in [14], when $m = 1$ and $k = 2$, the amplitude of magnetic flux density components corresponding to $q_{1,2}$ is the largest, thus the number of pole pairs in stator permanent magnet can be obtained.

For the stator, the expression of pole pairs of permanent magnet P_s can be expressed as follows:

$$
p_s = p + p_\omega
\tag{4}
$$

The angular velocity of the space harmonics of the flux density can be expressed as:

$$
\omega_{m,k} = p_\omega\omega_h + (-1)^k mp\omega_r
\tag{5}
$$

where ω_h is the angular velocity of the high-speed rotor.

Due to the coupling between the asynchronous space harmonics of torque transmission and the magnetic field generated by the stator, its rotation speed is zero ($\omega_{1,2} = 0$); therefore, the transmission ratio G_r can be derived from Eq. (5):

$$G_r = -\frac{p_\omega}{p} \tag{6}$$

where "$-$" represents the reverse output speed.

In this paper, there is only one cycle of the non-uniform air gap ($p_\omega = 1$), and the inner and outer PMs are arranged in a fan shape. The Halbach arrays are adopted for both of them. Its structure is shown in Fig. 3. Like a normal Halbach array, each pole permanent magnet is divided into two small pieces, but each small permanent magnet is changed from the original rectangular row into a triangular shape.
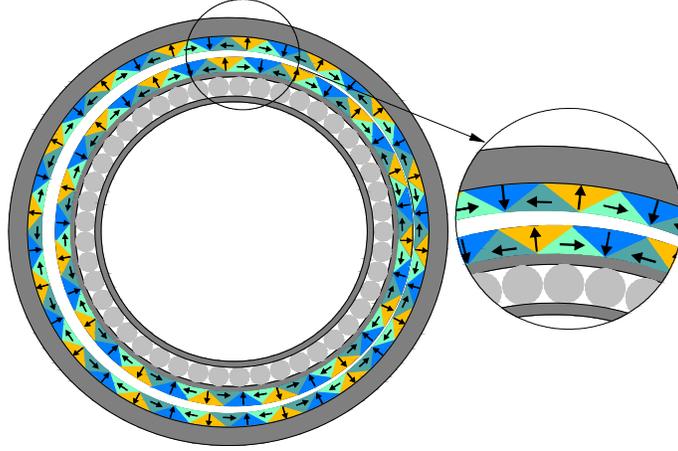
Figure 3. Proposed MHG.

2.2. Magnetic Field Analysis

In order to analyze the magnetic field characteristics of the proposed model, the MHG with a transmission ratio of $-15 : 1$ is established by *Ansys* finite element analysis software. The specific parameters are shown in Table 1, which are obtained according to experience and References [14] and [16].

Figure 4 shows the distributions of magnetic flux lines of two MHGs obtained by finite element simulation. It can be observed that the magnetic flux lines of the proposed MHG are obviously concentrated in the air gap, and the magnetic flux densities in the stator yoke and rotor yoke are greatly reduced. Therefore, the volume, cost, and weight can be reduced by diminishing the yoke materials.

Figure 5 shows the radial and tangential magnetic flux density waveforms in the middle air gap calculated by finite element analysis. It is obvious that the radial magnetic flux density and tangential magnetic flux density amplitudes of the air gap increase significantly.

Figure 6 shows the harmonic spectrum of flux density in the conventional MHG and proposed MHG. As can be seen from Fig. 6(a), there are mainly 14th, 15th, 16th, 44th, 45th, and 46th harmonics. We can know from [14], the 15 harmonics are the fundamental wave components, and the 14th, 15th, and 16th harmonics are conducive to the establishment of electromagnetic torque, which is the effective harmonics. The 45th harmonics are the third harmonic component (15×3), and the 44th, 45th, and 46th harmonics are not involved in the establishment of electromagnetic torque. After the improvement, the amplitude of the 14th, 15th and 16th harmonic components of the magnetic gear is significantly increased, while the amplitude of the 44th, 45th, and 46th harmonic components is decreased.

In the same way, the tangential magnetic density harmonic distribution can be obtained by Fourier decomposition of tangential magnetic density, as shown in Fig. 6(b). The tangential harmonics have

(a)   (b)
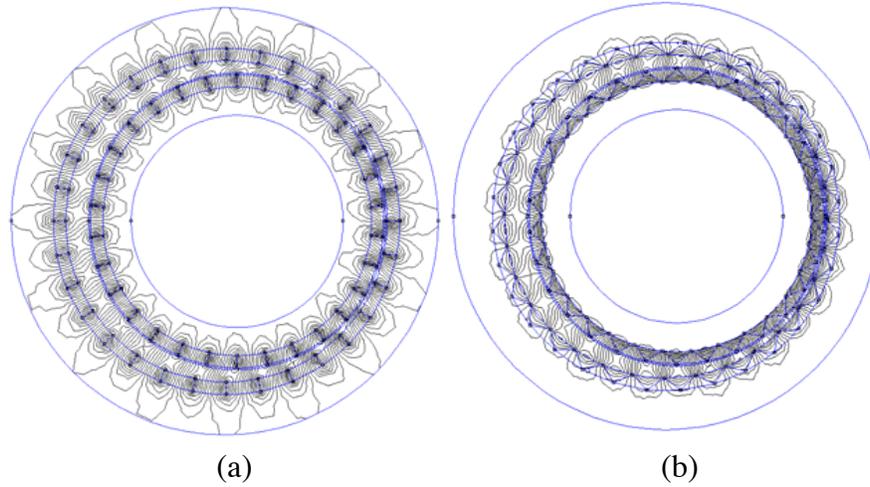
Figure 4. Flux line distributions. (a) Conventional, (b) proposed.

Table 1. Parameters of MHG.

Parameters	Values
Outer radius of stator yoke (mm)	54
Inner radius of stator yoke (mm)	49
Outer radius of low-speed rotor yoke (mm)	41.5
Inner radius of low-speed rotor yoke	36.5
Thickness of stator PMs (mm)	3.5
Thickness of low-speed rotor PMs (mm)	3.5
Eccentric distance (mm)	3
Pole pairs of stator	16
Pole pairs of low-speed rotor	15
The minimum air gap (mm)	1
The maximum air gap (mm)	7
Remanence of PMs (T)	1.25
Relative permeability	1
Average air gap length (mm)	4
Axial length (mm)	40
PMs material	NdFeB

14th, 15th, 16th, 44th, 45th, and 46th harmonics. It is obvious that the amplitude of the 14th, 15th, and 16th harmonic components of the proposed MHG is increased, while the amplitude of the 44th, 45th, and 46th harmonic components is slightly decreased.

3. TORQUE

3.1. Cogging Torque Optimization in PMSM Portion

Static torque is one of the important properties of magnetic gear. The low-speed rotor is rotated around the stator center for one electrical cycle to obtain the torque characteristics in the air gap. According to the Maxwell tensor method, in the two-dimensional coordinate system, the closed surface is selected
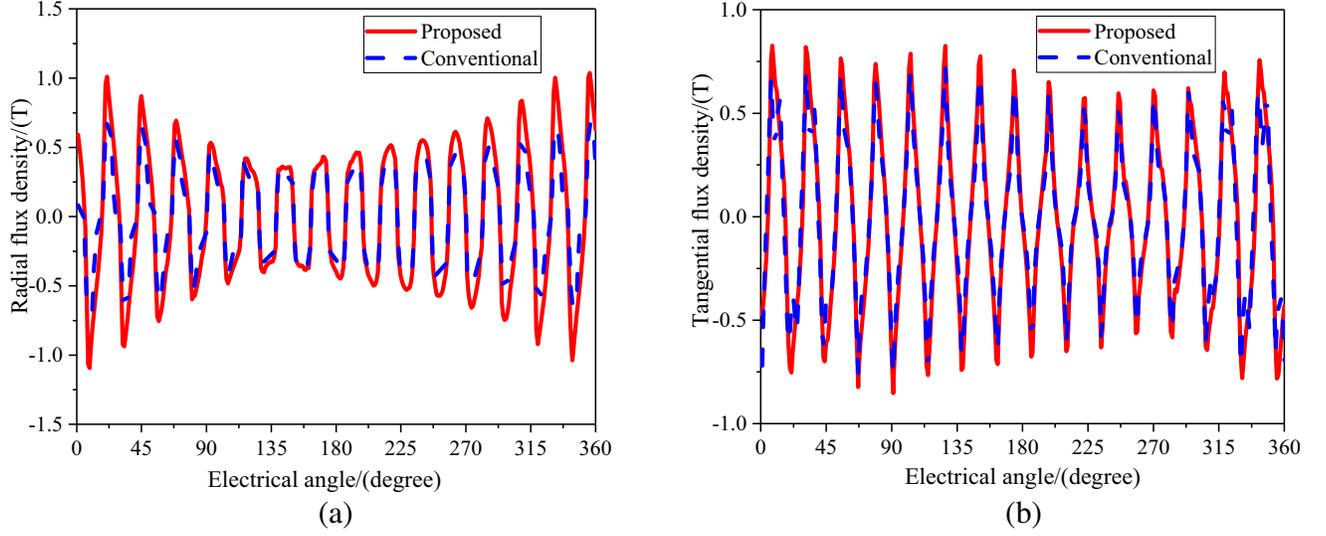
Figure 5. Flux density waveforms. (a) Radial component; (b) tangential component.
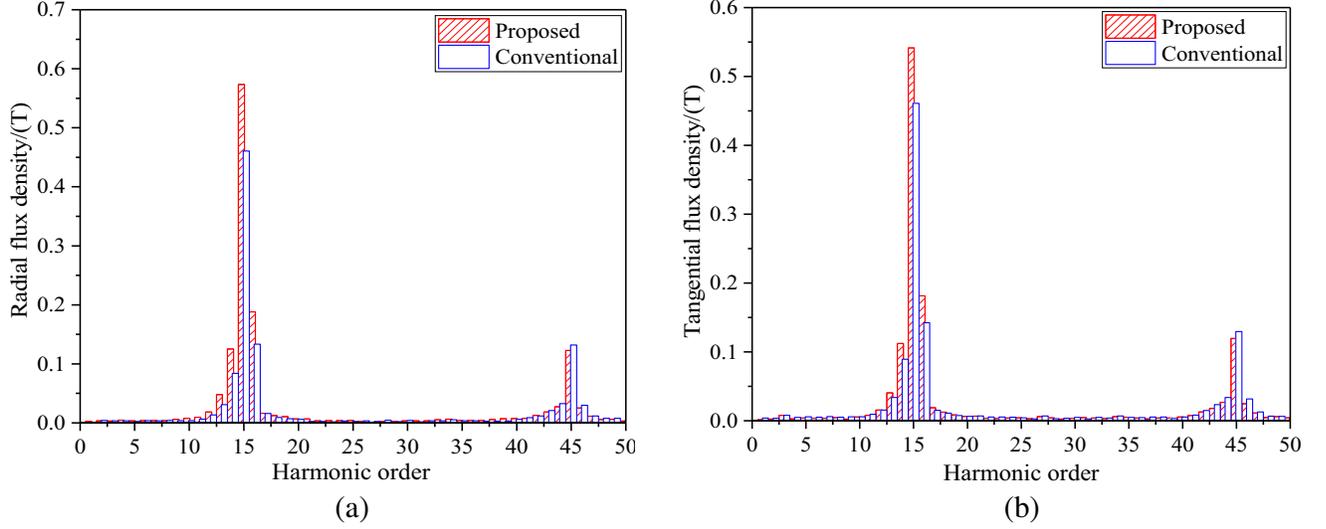
Figure 6. Harmonic spectrum of flux densities in the air gap. (a) Radial component; (b) tangential component.

as the cylinder passing through the air gap. Through the coordinate transformation, the expressions of the radial electromagnetic force and tangential electromagnetic force are expressed as follows,

$$F_r = L_{ef}r \int_0^{2\pi} \frac{1}{2\mu_0}(B_r^2 - B_\theta^2)\mathrm{d}\theta \tag{7}$$

$$F_\theta = L_{ef}r \int_0^{2\pi} \left(\frac{1}{\mu_0}B_r B_\theta\right) \mathrm{d}\theta \tag{8}$$

where B_r and B_θ are the radial and tangential components of air gap magnetic flux density at radius r, respectively. L_{ef} is the axial length of the MHG, and r is the arbitrary circumference radius with the center of the low-speed rotor as the center in the air gap.

So, the electromagnetic torque of MHG is given by,

$$T = \frac{L_{ef}r^2}{\mu_0} \int_0^{2\pi} (B_r B_\theta)\mathrm{d}\theta \tag{9}$$

Figure 7 shows the static torques of the conventional and proposed MHGs at various values of torque angle.

It can be seen from Fig. 7 that the static torque waveforms of the two MHGs are all sinusoidal waves. When the rotation angle of the low-speed rotor is 180°, the static torque reaches the maximum value. The maximum static torques of the two kinds of MHG are 22.2 N·m and 40.26 N·m, respectively. The torque of the proposed model is 81.3% higher than that of the conventional MHG. Therefore, the torque density of the proposed MHG is increased by 81.3% in the same volume.
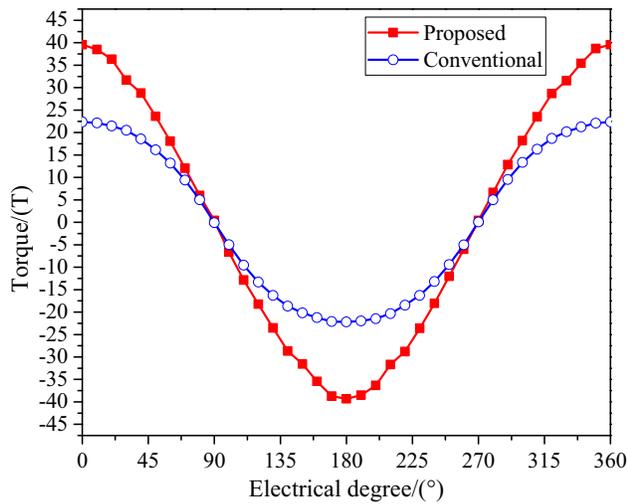
Figure 7. Static torque-angle curve.
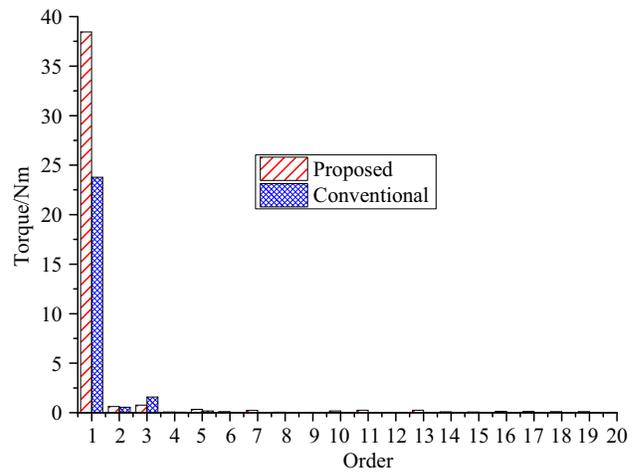
Figure 8. Harmonic spectrum of torque.

Figure 8 shows the harmonic spectrum of static torque. It can be seen that the fundamental wave increases greatly while the harmonic wave decreases greatly. It is further proved that the structure has better torque improvement.

Figure 9 shows the torque curve on the low-speed rotor, which changes with the rotation of the high-speed rotor. The low-speed rotor was rotated from 0° to 22.5° around the stator center with each rotation of 1.25°, and there were 19 calculation points. The maximum transmission torque of each point
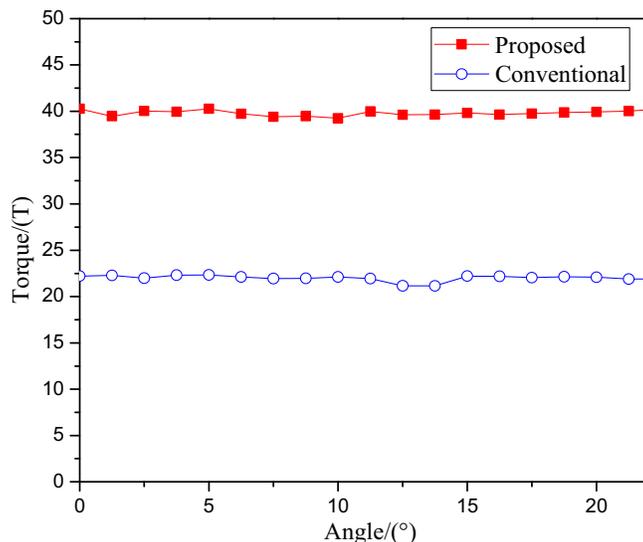
Figure 9. Variation of the maximum torque-angle curve.

was calculated, respectively. As can be seen from Fig. 8, the torque fluctuation range of the conventional model is 21.15 N·m to 22.34 N·m, while the torque fluctuation range of the proposed model is 39.25 N·m to 40.26 N·m. The torque ripples of the two MHG models are 5% and 2.5%, respectively. It is obvious that the output torque of the model is better in terms of stability.

4. CONCLUSION

In this paper, an MHG with double fan-shapes is proposed. The PMs on the low-speed rotor and the stator are arranged in a fan-shape and magnetized by a Halbach array. The model is established, and the two-dimensional finite element analysis is carried out. Compared with the conventional MHG, the air gap magnetic field and torque are calculated. It is found that the proposed MHG significantly enhanced the air-gap magnetic density, effectively reduced the harmonic content, and increased the static torque by 81.3%. Meanwhile, the output torque was more stable.

REFERENCES

1. Chen, M., K.-T. Chau, W. Li, C. Liu, and C. Qiu, "Design and analysis of a new magnetic gear with multiple transmission ratios," *IEEE Trans. Appl. Supercond.*, Vol. 3, No. 24, 1–4, 2014.
2. Jing, L. B., L. Liu, M. Xiong, and D. Feng, "Parameters analysis and optimization design for a concentric magnetic gear based on sinusoidal magnetizations," *IEEE Trans. Appl. Supercond.*, Vol. 5, No. 24, 1–5, 2014.
3. Liu, C. T., K. Y. Hung, and C. C. Hwang, "Developments of an efficient analytical scheme for optimal composition designs of tubular linear magnetic-geared machines," *IEEE Trans. Magn.*, Vol. 52, No. 7, 2016.
4. Man, Y., Y. Zhao, and C. Bian, "A kind of magnetic gear with high speed ratio," *Proceedings 3rd International Conference on Information Sciences and Interaction Sciences*, 632–634, 2010.
5. Shen, J. X., H. Y. Li, H. Hao, and M. J. Jin, "A coaxial magnetic gear with consequent-pole rotors," *IEEE Trans. Energy Convers.*, Vol. 32, No. 1, 267–275, 2017.
6. Li, K., S. Modaresahmadi, W. Williams, J. Bird, J. Wright, and D. Barnett, "Electromagnetic analysis and experimental testing of a flux focusing wind turbine magnetic gearbox," *IEEE Trans. Energy Convers.*, Vol. 34, No. 3, 1512–1521, 2019.
7. Desvaux, M., B. Multon, H. B. Ahmed, S. Sire, A. Fasquelle, and D. Laloy, "Gear ratio optimization of a full magnetic indirect drive chain for wind turbine applications," *2017 Twelfth International Conference on Ecological Vehicles and Renewable Energies (EVER)*, 11–13, 2017.
8. Park, C. B. and G. Jeong, "Design and analysis of magnetic-geared permanent magnet synchronous motor for driving electric vehicles," *2017 20th International Conference on Electrical Machines and Systems (ICEMS)*, 11–14, 2017.
9. Fang, Y. and T. Zhang, "Vibroacoustic characterization of a permanent magnet synchronous motor powertrain for electric vehicles," *IEEE Trans. Energy Convers.*, Vol. 33, No. 1, 272–280, 2017.
10. Golovanov, D., M. Galea, and C. Gerada, "High specific torque motor for propulsion system of aircraft," *International Conference on Electrical Systems for Aircraft*, 2–4, 2016.
11. Bruzzese, C., E. Ruggeri, M. Rafiei, D. Zito, T. Mazzuca, and G. Lipardi, "Mechanical arrangements onboard ship of innovative permanent magnet linear actuators for steering gear," *2017 International Symposium on Power Electronics*, 19–21, 2017.
12. Atallah, K. and D. Howe, "A novel high-performance magnetic gear," *IEEE Trans. Magn.*, Vol. 37, No. 4, 2844–2846, 2001.
13. Rens, J., K. Atallah, S. D. Calverley, and D. Howe, "A novel magnetic harmonic gear," *2007 IEEE International Electric Machines & Drives Conference*, 698–703, Antalya, 2007. DOI: 10.1109/iemdc.2007.382752.
14. Rens, J., K. Atallah, S. D. Calverley, and D. Howe, "A novel magnetic harmonic gear," *IEEE Trans. Ind. Appl.*, Vol. 46, No. 1, 206–212, 2010.

15. Jorgensen, F. T., T. O. Andersen, and P. O. Rasmussen, "The cycloid permanent magnetic gear," *IEEE Trans. Ind. Appl.*, Vol. 44, No. 6, 1659–1665, 2008.

16. Zhang, Y., J. Zhang, and R. Liu, "Magnetic field analytical model for magnetic harmonic gears using the fractional linear transformation method," *Chinese Journal of Electrical Engineering*, Vol. 5, No. 1, 47–52, 2019.

17. Guo, B. C., Y. K. Huang, and F. Peng, "An analytical model for axial flux PM machines with Halbach array," *Proceedings of the Chinese Society of Electrical Engineering*, Vol. 39, No. 1, 289–295, 2019.

18. Xu, X. Z., Z. Sun, and X. D. Wang, "Characteristic of a novel PM linear synchronous motor with Halbacharray consequent-pole," *Transactions of China Electrotechnical Society*, Vol. 34, No. 9, 1825–1833, 2019.

19. Jian, L. N. and K. T. Chau, "A coaxial magnetic gear with Halbach PM arrays," *IEEE Trans. Energy Convers.*, Vol. 25, No. 2, 319–328, 2010.

20. Jing, L. B., T. Zhang, Y. Gao, R. Qu, Y. Huang, and T. Ben, "A novel HTS modulated coaxial magnetic gear with eccentric structure and Halbach arrays," *IEEE Trans. Appl. Supercond.*, Vol. 5, No. 29, 1–5, 2019.